DRAFT VERSION JULY 1, 2011
Preprint typeset using LaTeX style emulateapj v. 08/13/06

A 5 MICRON IMAGE OF β PICTORIS B AT A SUB-JUPITER PROJECTED SEPARATION: EVIDENCE FOR A MISALIGNMENT BETWEEN THE PLANET AND THE INNER, WARPED DISK

THAYNE CURRIE[1], CHRISTIAN THALMANN[2], SOKO MATSUMURA[3], NIKKU MADHUSUDHAN[4], ADAM BURROWS[4], MARC KUCHNER[1]

Draft version July 1, 2011

ABSTRACT

We present and analyze a new M' detection of the young exoplanet β Pictoris b from 2008 VLT/NaCo data at a separation of ≈ 4 AU and a high signal-to-noise rereduction of L' data taken in December 2009. Based on our orbital analysis, the planet's orbit is viewed almost perfectly edge-on ($i \sim 89$ degrees) and has a Saturn-like semimajor axis of $9.50\,\mathrm{AU}^{+3.93\,\mathrm{AU}}_{-1.7\,\mathrm{AU}}$. Intriguingly, the planet's orbit is aligned with the major axis of the outer disk ($\Omega \sim 31$ degrees) but probably misaligned with the warp/inclined disk at 80 AU often cited as a signpost for the planet's existence. Our results motivate new studies to clarify how β Pic b sculpts debris disk structures and whether a second planet is required to explain the warp/inclined disk.

Subject headings: stars: early-type, planetary systems, stars: individual β Pictoris

1. INTRODUCTION

Two decades of studies have argued that the nearby, 12 Myr-old A-type star β Pictoris likely harbors a young planetary system (e.g. Smith and Terrile 1984; Kalas and Jewitt 1995; Mouillet et al. 1997); recently, Lagrange et al. (2009a, 2010) detected a $\approx 9 \pm 3$ M_J planet around this star (β Pic b). Imaged at projected separations of ~ 6 AU and ~ 8 AU (November 2003 and October–December 2009, respectively), β Pic b – along with HR 8799e (Marois et al. 2010; Currie et al. 2011) – may also provide a more direct comparison to the solar system's gas giants than other directly imaged planets which are at wider separations (e.g. Fomalhaut b and HR 8799bcd Kalas et al. 2008; Marois et al. 2008). Current studies have yet to detect the planet at projected separations $\lesssim 0.3''$ (Lagrange et al. 2009b; Fitzgerald et al. 2009). Data at these smaller separations could provide crucial constraints on the planet's orbit.

Imaging planets at small, $< 0.3''$ separations requires significantly reducing quasi-static speckle noise and wavefront errors induced by imperfect AO corrections. Advanced observing/image processing techniques like *angular differential imaging* (ADI) coupled with PSF subtraction from a *locally optimized combination of images* (LOCI) algorithm (Marois et al. 2006; Lafreniere et al. 2007) significantly attenuate speckles and increase sensitivity. New instrumentation, such as the *Gemini Planet Imager* (GPI Macintosh et al. 2008), will achieve far superior wavefront control. Generally, these efforts focus on planet imaging in the near-IR. However, mid-IR imaging naturally overcomes some of these challenges as the achievable Strehl ratio is better and the planet-to-star contrast is most favorable. High-contrast imaging with Strehl ratios ≥ 0.9 can yield at least some planet detections close to the telescope diffraction limit (e.g. 2 λ/D for HR 8799d; Serabyn et al. 2010). Because M band imaging often achieves these high Strehl ratios (Minowa et al. 2010; Hinz et al. 2006), it may be a promising route for detecting very young and self luminous planets at small λ/D separations, despite a much higher sky background.

In this Letter, we report a detection of β Pic b at a separation of $\sim 0.21''$ extracted from archival M' band VLT/NaCo data taken in November 2008. We also present a high signal-to-noise L' detection of β Pic b from December 2009 data first published in Lagrange et al. (2010). We combine these data with recent data from Bonnefoy et al. (2011) and Quanz et al. (2010) to better constrain the orbit and atmosphere of β Pic b.

2. OBSERVATIONS AND DATA

Our study originates from the need to test the ADI/LOCI reduction pipeline first presented in Currie et al. (2010) and updated in Currie et al. (2011) at separations smaller than those where the pipeline had previously extracted planet signals ($r < 0.375''$). Because β Pic b's reported projected separation in 2009 was $\approx 0.3''$ (Lagrange et al. 2010), we chose the now publicly available Lagrange et al. L' band data from December 29, 2009 to test our code performance. Lagrange et al. (2010) discusses the details of the L' band observations. The total field rotation in units of the image FWHM was ~ 3 λ/D, sufficient for using our reduction pipeline.

Figure 1 (top-left panel) shows our processed L' band image using the LOCI algorithm in annular regions of 250×FWHM ($N_A = 250$) with reference images selected from frames with at least 0.5×FWHM field rotation ($\delta = 0.5$). The planet is easily detected and is well separated from residual speckle noise. The planet signal-to-noise, determined from the dispersion in pixel intensity values in concentric annuli, is SNR ~ 21: about a factor of 4–5 greater than from Lagrange et al. (2010).

Motivated by this success, we searched for additional β Pic data in the VLT/NaCo archive taken in ADI mode between 2003 and 2009, finding a set taken on November 11, 2008 with the L27 camera. Most of these data were taken in sparse aperture masking mode in K_s, L', and M' bands over a span of ~ 4 hours: these data were

[1] NASA-Goddard Space Flight Center
[2] Anton Pannekoek Institute, University of Amsterdam
[3] Department of Astronomy, University of Maryland-College Park
[4] Department of Astrophysical Sciences, Princeton University

mentioned in Lagrange et al. (2009b) as not providing good constraints on the companion. However, we found $\sim$ 13 minutes of the M' data taken in ADI mode without aperture masking at various times in between the masking data. Over the course of the entire observing sequence, the parallactic angle changed by $\sim$ 100 degrees, or $\sim$ 2.4–3 λ/D at 0.2″–0.25″: sufficient for image processing with our pipeline.

Basic image processing of the M' band data followed steps outlined in Currie et al. (2011). After registering each image and subtracting off the smooth seeing halo, we Fourier filtered the data to remove residual low spatial frequency noise and masked any hitherto unidentified bad pixels previously lost in the seeing halo. We explored a range of LOCI parameter space, varying δ, N_A, and the ratio of the radial to azimuthal lengths of the subtraction annulus (g). Because β Pic b is very luminous in the mid-IR (e.g. $\Delta L' \approx 7.7$; Lagrange et al. 2010, and Section 3 of this work), we focused on "aggressive" LOCI settings of δ = 0.25–0.5, N_A = 200-300, and g = 0.3–1, which better remove residual speckle noise.

Figure 1 (top-right panel) shows our best reduced M' image. β Pic b is clearly detected in the southwest quadrant $\approx$ 0.2–0.25″ from the star (SNR $\sim$ 6). Manually inspecting each image between the radial profile subtraction and final image combination steps and examining a signal-to-noise map of the median-combined image also shows that the peak does not result from latent image artifacts. Slightly different settings for δ, N_A, and g also yield significant detections (bottom panels).

3. ANALYSIS

Our new M' band detection and high signal-to-noise L' band detection allow new constraints on the planet's orbit. To derive precise astrometry needed to investigate the planet's orbit, we adopt the NaCo plate scale and orientation for the L27 camera from Bergfors et al. (2011): 27.1 mas/pixel and a north position angle of -0.6 degrees. These values are nearly identical to those for the L27 camera quoted by Lagrange et al. (2009a) for 2003 NaCo data and for the S27 camera from Ehrenreich et al. (2010) calibrated from Trapezium data acquired closest in time to the β Pic data: our astrometric results does not leverage on which calibration we use.

To fine tune our measurements, we correct for the photometric and astrometric bias induced by LOCI processing by comparing the imputed fluxes and positions of fake point sources added to registered images with computed fluxes and centroid positions obtained after LOCI processing (e.g. Lafreniere et al. 2007; Thalmann et al. 2009; Currie et al. 2011). While we lack unsaturated data from this run to directly confirm the PSF shape, unsaturated M' data taken in prior runs such as that for HD 158882 (March 2007) show that the AO-assisted NaCo M' PSF core is axisymmetric and well reproduced by a simple Gaussian intensity distribution. For the L' band data, the astrometric bias is minimal, whereas β Pic b's measured radial separation in M' band is biased by about +0.5 pixels (0.013"). The position angle offsets for both data were minimal.

We determine the M' band position to be at a separation of r = 0.210 $\pm$ 0.027″ and position angle of 211.49 $\pm$ 1.9 degrees. The L' band position is at 0.326 $\pm$ 0.013″ and 210.64 $\pm$ 1.2 degrees (Table 1). Here we conservatively assume an uncertainty in radial separation of one pixel for M' band and 0.5 pixels for the (higher signal-to-noise) L' band data. The position angle uncertainty – determined from the dispersion in values using different centroiding estimates (e.g. cntrd.pro vs. gcntrd.pro) is 0.25 pixels (0.7 mas×r), or 1.2 and 1.9 degrees for L' and M', comparable to uncertainties for β Pic b by Lagrange et al. (2009a, 2010) and Bonnefoy et al. (2011). Assuming that β Pic is 19.3 pc distant (Crifo et al. 1997), the planet was at a projected separation of 4.05 $\pm$ 0.50 AU on November 11, 2008 and 6.29 $\pm$ 0.25 AU on December 29, 2009.

To determine the range of allowable orbits for β Pic b, we follow the method described in Janson et al. (2011) used to model the orbit of the low-mass brown dwarf companion GJ 758 B (Thalmann et al. 2009; Currie et al. 2010), somewhat similar to earlier analyses for β Pic b (Lagrange et al. 2009b; Fitzgerald et al. 2009). In this approach, we perform a Monte Carlo simulation comparing the astrometry to predictions from randomly selected orbits, where we allow all orbital parameters to vary. The minimum χ^2 value in our simulation is $\chi^2 \sim$ 1.23. Given our data's weak constraints on the orbital acceleration and the degeneracies due to the unknown line-of-sight components of planet position and velocity, no single 'best' orbital solution emerges. Rather, the best-fitting solutions describe an extended, well- defined family of solutions that all match the data equally well. We choose a cut of $\chi^2 \leq 2.23$ ($\chi^2 \lesssim \chi^2_{\rm min} + 1$) to represent the family of best-fitting orbits. We also consider the results for a cut of $\chi^2 \leq 8$ (χ^2 for a 1-σ deviation in each of the data's degrees of freedom): a family of 'average-fitting' solutions. From the set of models satisifying this criterion, we determine the median value of each parameter, weighted by the ratio of the mean to current orbital velocity for the corresponding orbit, and identify the weighted 68% confidence interval about the median. We include astrometry from the highest signal-to-noise data separated in time by more than $\sim$ 3 months (Table 1).

Figures 2 and 3 displays our Monte Carlo simulation results. For a $\chi^2 \leq 2.23$ cutoff (Figure 2), the range of best-fit orbital parameters (weighted median, [weighted 68% confidence interval]) include a_p = 10.99 [8.18, 15.88] AU, i = 89.47 [89.19, 89.69] degrees, e = 0.12 [0.03,0.31], and Ω = 30.89 [30.57, 31.17] degrees. For nearly circular orbits ($e < 0.1$), the range in semimajor axes is much narrower ($a_p \sim$ 8–12 AU). If we relax our fitting criteria to accept models with $\chi^2 \leq 8$ (Figure 3), we find a_p = 9.50 [7.80, 13.43] AU and e = 0.10 [0.02,0.23]. More importantly, the inclination and longitude of ascending node are still nearly single valued: i = 88.93 [88.06, 89.40] and Ω = 31.32 [30.56, 32.12]. Thus, β Pic b's orbit must be viewed almost perfectly edge on, consistent with that for β Pic's debris disks, with a north position angle of $\sim$ 30.8 degrees for the outer debris disk (Kalas and Jewitt 1995, see also Boccaletti et al. 2009) but inconsistent with the inner disk position angle, which is offset by $\sim$ 5 degrees (Heap et al. 2000; Golimowski et al. 2006).

Unfortunately, the M' band observations of β Pic were taken with the star saturated within $\sim$ 3 pixels ($\sim$ 0.6 FWHM) of the centroid and there were likewise no unsaturated standard star observations. We derive a very

crude magnitude estimate by scaling the M' PSF of HD 158882 to the unsaturated portion of the β Pic PSF and use HD 158882's known brightness (K_s = 5.09; K_s-M' $\sim$ 0) to calibrate β Pic b's brightness. We estimate $\Delta M'$ $\approx$ 8.02 $\pm$ 0.50 ($M_{M'}$ $\approx$ 9.99), where we consider the uncertainties in our PSF fitting scaling, the dispersion in individual planet magnitude estimates drawn from separate reductions, and the intrinsic signal-to-noise of our detection. We determine an L' contrast of $\Delta L' = 7.71 \pm 0.06$. Combining the L' measurement with the K_s band and [4.05] data from Bonnefoy et al. (2011) and Quanz et al. (2010), we have three good quality photometric points to investigate the family of possible solutions for β Pic b's atmospheric properties.

Figure 4 compares the β Pic b photometry to best-fit spectra for models with log(g) = 3.5/4–4.5 and T_{eff} = 1000–1800 K for a range of cloud prescriptions: the Model A and AE thick cloud prescriptions respectively from Currie et al. (2011) and Madhusudhan et al. (2011) that best fit the HR 8799 planet SEDs, the Model E cloud deck prescription appropriate for brown dwarfs (Burrows et al. 2006), and a cloudless atmosphere. The χ^2_ν values for these models are, respectively, χ^2_ν = 24.8, 12.3, 20.4, and 43.2 for Models A, AE, E, and the cloudless case. The AE thick cloud model provides the best fit. Thick cloud models also produce redder L'-M' colors at high temperatures, similar to that estimated here ($\approx$ -0.22 $\pm$ 0.50), though our lack of a reliable M' photometric calibration precludes strong conclusions. Good photometry is available in only three filters, so we cannot yet say that β Pic b has thick clouds like the HR 8799 planets (Currie et al. 2011; Madhusudhan et al. 2011).

The range of gravities and effective temperatures are log(g) = 3.5–4.5 and T_{eff} = 1400–1800 K. The implied masses for these models range between 4.1 M_J and 19.2 M_J and ages range between 1 and 27 Myr, broadly consistent with the planet mass (9 $\pm$ 3 M_J; Lagrange et al. 2010), stellar age (12 Myr; Zuckerman et al. 2001), and likely formation timescale ($\leq$ 3–5 Myr; Currie et al. 2009). Planet fluxes in the near-IR (1–1.65 μm) and the 3–3.5 μm methane absorption trough are highly sensitive to cloud structure (e.g. Currie et al. 2011; Madhusudhan et al. 2011). Thus, J or H broadband data and/or narrowband 3–3.5 μm data will be critical in breaking model fitting degeneracies.

4. DISCUSSION

We present a new detection of β Pic b in M' band at a separation of $\sim 0.21''$ ($a_{\rm projected}$ = 4.05 AU) from archival VLT/NaCo data taken in November 2008 and a high SNR rereduction of L' data first reported by Lagrange et al. (2010), using these data to constrain the planet's orbit and atmospheric properties. For orbits whose fit to the data yield $\chi^2 \leq 2.23$, we find that the β Pic planet has a semimajor axis of a_p = 10.99 $\rm AU^{+4.69AU}_{-2.81AU}$ and a moderate/low eccentricity ($e \lesssim 0.31$). Admitting orbital solutions with $\chi^2 \leq 8$, the parameter ranges are a_p = 9.50 $\rm AU^{+3.93AU}_{-1.7AU}$ and e $\lesssim$ 0.23. In both cases, values for the planet's inclination (i $\sim$ 88.06–89.69 degrees) and longitude of ascending node ($\Omega \sim$ 30.56–32.12 degrees) are tightly constrained and imply that the planet's orbit is almost perfectly aligned with the outer debris disk, but not the inclined inner disk ($\Omega \sim$ 35–36 degrees). We cannot extract reliable photometry from our M' band data; new data at 1–1.65 μm and $\sim$ 3–3.5 μm is needed to constrain β Pic b's atmosphere.

Numerous studies of the β Pic debris disk(s) have identified the star as harboring a young planetary system (e.g. Smith and Terrile 1984; Kalas and Jewitt 1995; Mouillet et al. 1997; Weinberger et al. 2003). More recently, the presence of a warp in the disk at $\sim$ 80 AU – due to the combined effects of the main disk with PA $\sim$ 30.8 and a second, inclined disk offset by 5 degrees – was identified as a clear signpost of a perturbing planet (e.g. Mouillet et al. 1997; Heap et al. 2000; Golimowski et al. 2006), motivating high-contrast imaging studies to image the planet. Lagrange et al. (2009a) identified β Pic b as a likely source of the inclined disk and used the disk morphology to derive mass estimates (see also Lagrange et al. 2010).

Our results suggest that β Pic b is probably *not* aligned with the inner disk/warp but rather the main disk, as the allowed range in Ω is offset from the main disk as measured by Kalas and Jewitt (1995) by no more than $\sim$ 1 degree. Furthermore, the planet may be misaligned with the submm disk emission (Wilner et al. 2011), which is sensitive to dynamical sculpting by planets (Kuchner and Stark 2010). However, models accounting for the inclined inner disk presume that the planet's orbit is also inclined relative to the main disk (e.g. Mouillet et al. 1997; Augereau et al. 2001). New beta Pic b astrometry, a more precise astrometric calibration of existing beta Pic NaCo data by determining and correcting for image distortion, and a detailed relative calibration between NaCo data and data revealing the disk will further clarify how beta Pic b's orbital plane compares to that for the main disk and the inner disk/warp. Furthermore, our new orbital constraints for β Pic b strongly motivate new studies of the dynamical sculpting of β Pic's debris disk by planets. If β Pic b or non-planet related mechanisms (e.g. Armitage and Pringle 1997) fail to explain the inclined debris disk/warp, the existence of additional planets in the system may be required.

Our M' band detection demonstrates that it is possible to directly image planets at separations approaching the telescope diffraction limit without sparse aperture masking interferometry (SAM; Ireland and Kraus 2008). The high Strehl ratio, large amount of field rotation, large mid-IR planet brightness, and LOCI processing pipeline are the keys to closing this gap. While SAM can detect planets interior to the telescope diffraction limit, it is overall less sensitive. However, the techniques can be complementary, yielding detections or robust limits on infant gas giant planets around the youngest stars on $\sim$ 5–100 AU scales.

Upcoming facilities like GPI, SPHERE, SCExAO, and Project 1640 achieve higher contrast at small inner working angles in the near-IR primarily through more sophisticated wavefront control (Macintosh et al. 2008; Beuzit et al. 2008; Martinache and Guyon 2009; Hinkley et al. 2011). Our results, coupled with previous L' band detections of β Pic from Lagrange et al. (2009a, 2010) and the high signal-to-noise L' band detection of HR 8799e (Marois et al. 2010) suggest that the mid-IR may also be fertile ground for new exoplanet detections at small separations for very young systems. Young, nearby 1.5–2 $M_\odot$ stars like β Pic are particularly promising targets

TABLE 1
β Pic Data Used in this Paper

Astrometry			
Date	Filter	Separation ($''$),Position Angle ($^\circ$)	Reference
11-10-2003	L'	0.411 ± 0.008, 31.7 ± 1.3	Lagrange et al. (2009a)
11-11-2008	M'	0.210 ± 0.027, 211.49 ± 1.9	this work
12-29-2009	L'	0.326 ± 0.013, 210.64 ± 1.2	this work
03-20-2010	K_s	0.345 ± 0.012, 209.8 ± 0.8	Bonnefoy et al. (2011)
Photometry			
Date	Filter	Absolute Magnitude	Reference
03-20-2010	K_s	11.20 ± 0.12	Bonnefoy et al. (2011)
12-29-2009	L'	9.73 ± 0.06	this work
04-03-2010	[4.05]	9.77 ± 0.23	Quanz et al. (2010)
11-11-2008	M'	$\approx 9.99 \pm 0.50$	this work

NOTE. — Our astrometry and photometry are drawn from the three separate reductions shown in Figure 1. The L' measurement assumes $L'_{\beta,\ Pic} = 3.45$. The M' photometry lacks reliable photometric calibration and thus is not useful for atmospheric modeling.

for direct imaging surveys (e.g. Crepp and Johnson 2011) and many have resolved debris disks (e.g. HD 181327, Schneider et al. 2006; Chen et al. 2008). Imaging massive planets in such systems can yield additional studies of planet-disk interactions, such as those motivated by this work.

We thank David Ehrenreich, Karl Stapelfeldt, Scott Kenyon, Justin Crepp, and the anonymous referee for suggested improvements to the manuscript and Michael McElwain, Sally Heap, Sarah Maddison, and Aki Roberge for other useful discussions. TC is supported by a NASA Postdoctoral Fellowship. AB is supported in part under NASA ATP grant NNX07AG80G, HST grant HST-GO-12181.04-A, and JPL/Spitzer Agreements 1417122, 1348668, and 1371432. SM is supported by an Astronomy Center for Theory and Computation Prize Fellowship.

REFERENCES

Armitage, P., Pringle, J., 1997, ApJ, 488, 47L
Augereau, J. C., 2001, A&A, 370, 440
Bergfors, C., et al., 2011, A&A, 528, 134
Beuzit, J.-L., et al., 2008, SPIE, 7014, 41
Boccaletti, A., et al., 2009, A&A, 495, 523
Bonnefoy, M., et al., 2011, A&A, 528, 15L
Burrows, A., et al., 2006, ApJ, 640, 1063
Chen, C., Fitzgerald, M., Smith, P., 2008, ApJ, 689, 539
Crepp, J., Johnson, J., 2011, ApJ, 733, 126
Crifo, F., et al., 1997, A&A, 320, 29L
Currie, T., Lada, C. J, et al., 2009, ApJ, 698, 1
Currie, T., et al., ApJ, 721, 177L
Currie, T., Burrows, A., et al., 2011, ApJ, 729, 128
Ehrenrieich, D., et al., 2010, A&A, 523, 73
Fitzgerald, M., et al., 2009, ApJ, 706, 41L
Golimowski, D., et al., 2006, AJ, 131, 3109
Heap, S., et al., 2000, ApJ, 539, 435
Hinkley, S., et al., 2011, PASP, 123, 74
Hinz, P., et al., 2006, ApJ, 653, 1486
Ireland, M., Kraus, A., 2008, ApJ, 678, 59L
Janson, M., et al., 2011, ApJ, 728, 85
Kalas, P., Jewitt, D., 1995, AJ, 110, 794
Kalas, P., et al., 2008, Science, 322, 1345
Kuchner, M., Stark, C., 2010, AJ, 140, 1007
Lafreniere, D., et al., 2007, ApJ, 660, 770
Lagrange, A.-M., et al., 2009a, A&A, 493, 21L
Lagrange, A.-M., et al., 2009b, A&A, 506, 927
Lagrange, A.-M., et al., 2010, Science, 329, 57
MacIntosh, B., et al., 2008, SPIE, 7015, 31
Madhusudhan, N., Burrows, A., Currie, T., 2011, ApJ in press, arXiv:1102.5089
Marois, C., et al., 2006, ApJ, 641, 556
Marois, C., et al., 2008, Science, 322, 1348
Marois, C., et al., 2010, Nature, 468, 1080
Martinache, F., Guyon, O., 2009, SPIE, 7440, 20
Minowa, Y., et al., 2010, SPIE, 7736, 122
Mouillet, D., et al., 1997, MNRAS, 292, 896
Quanz, S., et al., 2010, ApJ, 722, 49L
Schneider, G., et al., 2006, ApJ, 650, 414
Serabyn, E., et al., 2010, Nature, 464, 1018
Smith, B., Terrile, R. J., 1984, Science, 226, 1421
Thalmann, C., et al., 2009, ApJ, 707, 123L
Weinberger, A., Becklin, E. E., Zuckerman, B., 2003, ApJ, 584, 33L
Wilner, D., Andrews, S., Hughes, A. M., 2011, ApJ, 727, 42L
Zuckerman, B., et al., 2001, ApJ, 562, 87L

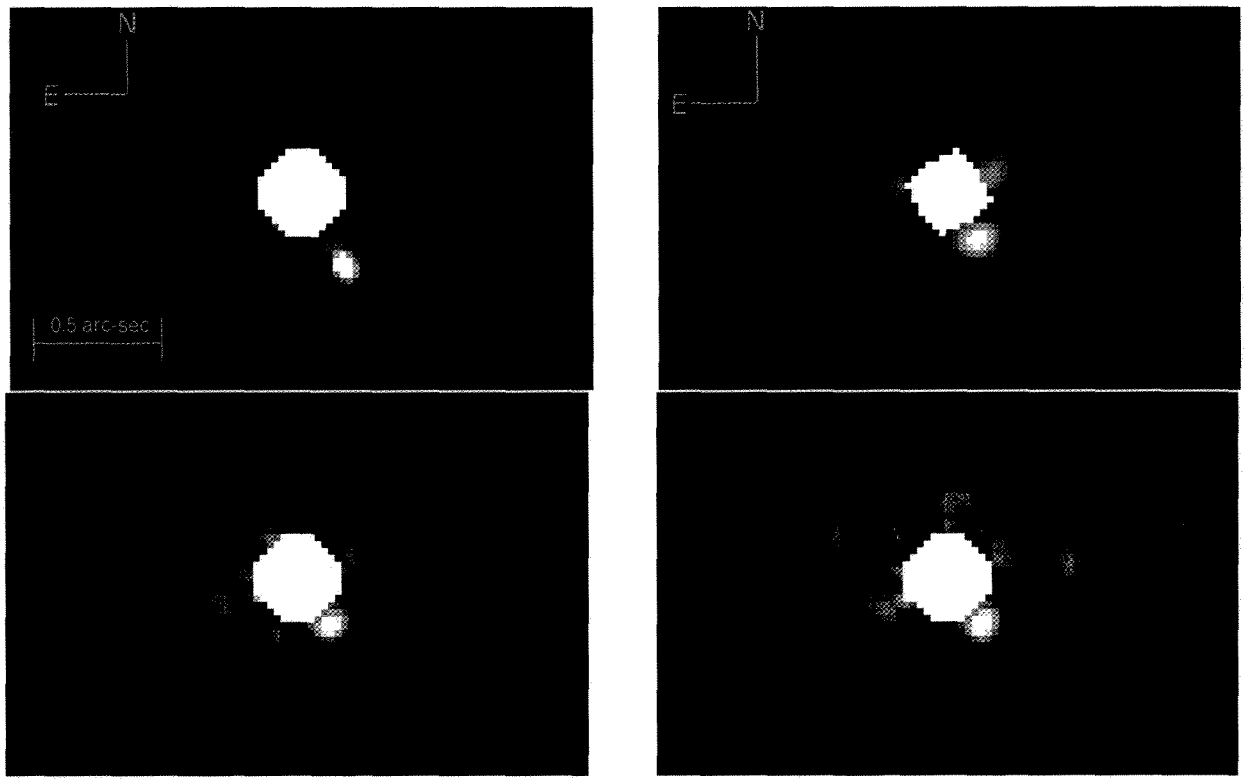

FIG. 1.— (Top-left) Reduced VLT/NaCo L' band image from Dec. 29, 2009 data showing a 21-σ detection of β Pic b at a separation of ~ 0.32". (Top-right) Reduced image showing the detection of β Pic b in M' band (same image size). The LOCI parameters used to construct the reduced image include $\delta = 0.25$, $g = 0.4$, and $N_A = 250\times$FWHM. (Bottom panels) Reduced images using less aggressive LOCI settings – $\delta = 0.5$, g=0.5, and $N_A = 300\times$FWHM (left panel) and $\delta = 0.5$, g=1, and $N_A = 300\times$FWHM (right panel) – yielding detections of SNR ~ 5 and 4.5, respectively. In general, we detect the β Pic planet at a 4–6 σ level using a range of LOCI parameters: δ = 0.25–0.5, g = 0.3–1, N_A = 200–300.

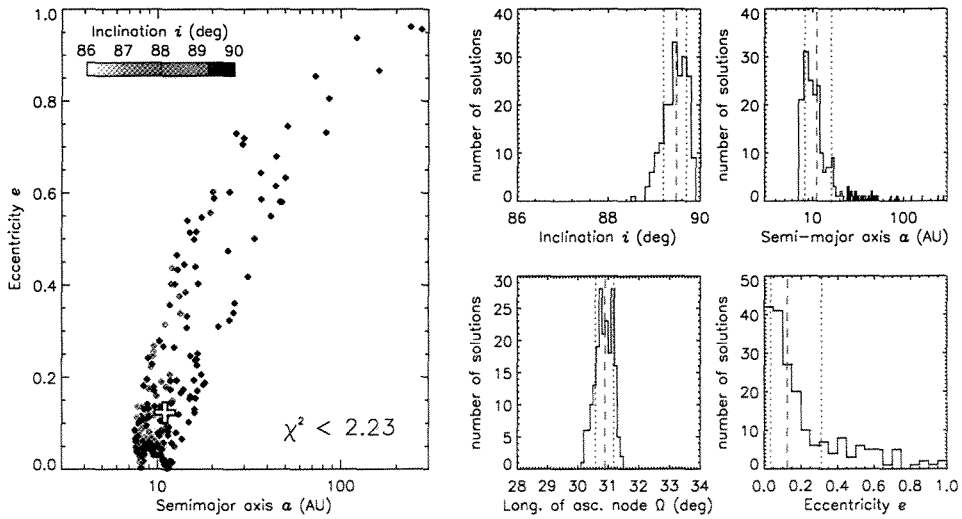

FIG. 2.— Orbital analysis results following the Monte Carlo method outlined in Thalmann et al. (2009), showing parameters for solutions fulfilling $\chi^2 \leq 2.23$. The left panel displays the family of solutions in semimajor axis, eccentricity, and inclination space. The right panels show histogram distributions of these three parameters and the longitude of the ascending node. The vertical dashed line identifies the weighted median value for each parameter; the vertical dotted lines define the 68% confidence interval for each parameter.

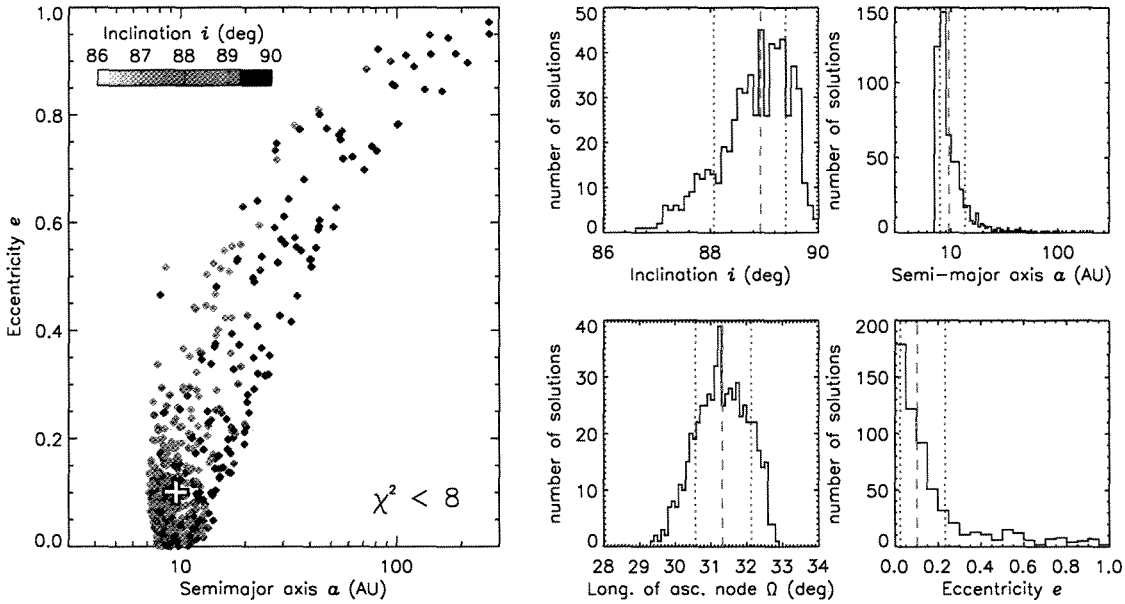

FIG. 3.— Same as previous figure except for orbital solutions fulfilling $\chi^2 \leq 8$.

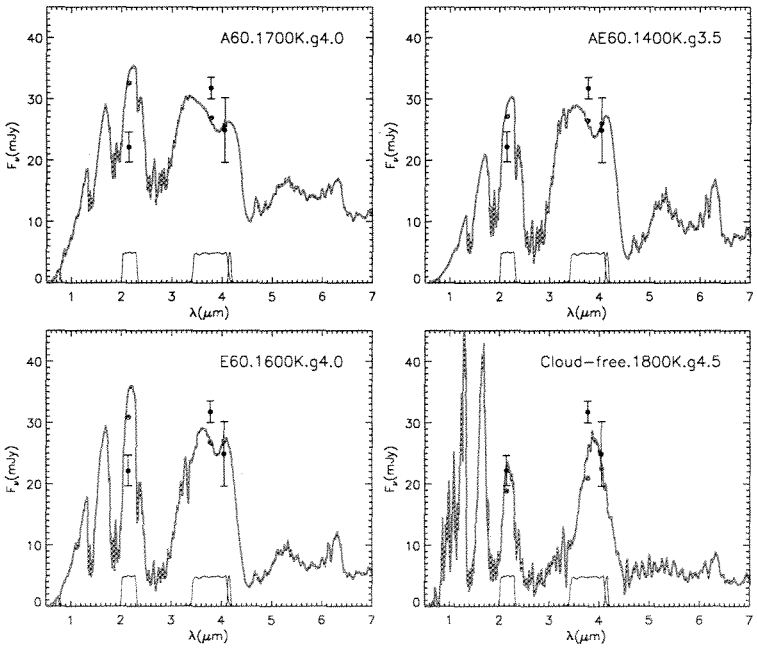

FIG. 4.— Figures comparing the β Pic b photometry to spectra for a range of cloud prescriptions: the Model A 'thick cloud' limit used in Currie et al. (2011) (upper-left), the Model AE 'thick cloud' prescription from Madhusudhan et al. (2011) (upper-right), the Model E brown dwarf cloud prescription from Burrows et al. (2006) (lower-left), and a cloud-free atmosphere also from Burrows et al. (2006) (lower-right). The blue dots show the flux predictions for each bandpass. All models assume a modal particle size of 60 μm.